The Astrophysical Journal, 649: L145–L147, 2006 October 1

THE TRAVELING-WAVE MRI IN CYLINDRICAL TAYLOR-COUETTE FLOW: COMPARING WAVELENGTHS AND SPEEDS IN THEORY AND EXPERIMENT

Günther Rüdiger
Astrophysikalisches Institut Potsdam, An der Sternwarte 16, D-14482 Potsdam, Germany; gruediger@aip.de
Rainer Hollerbach
Department of Applied Mathematics, University of Leeds, Leeds LS2 9JT, UK; rh@maths.leeds.ac.uk
Frank Stefani, Thomas Gundrum, and Gunter Gerbeth
Forschungszentrum Rossendorf, P.O. Box 510119, D-01314 Dresden, Germany; f.stefani@fz-rossendorf.de, th.gundrum@fz-rossendorf.de, g.gerbeth@fz-rossendorf.de
and
Robert Rosner
Department of Astronomy and Astrophysics, University of Chicago, Chicago, IL 60637; rrosner@astro.uchicago.edu
Received 2006 July 1; accepted 2006 August 15; published 2006 September 11

ABSTRACT

We study experimentally the flow of a liquid metal confined between differentially rotating cylinders, in the presence of externally imposed axial and azimuthal magnetic fields. For increasingly large azimuthal fields a wavelike disturbance arises, traveling along the axis of the cylinders. The wavelengths and speeds of these structures, as well as the field strengths and rotation rates at which they arise, are broadly consistent with theoretical predictions of such a traveling-wave magnetorotational instability.

Subject headings: instabilities — MHD — waves

1. INTRODUCTION

The magnetorotational instability (MRI) arises in a broad range of astrophysical problems, most importantly in accretion disks, where it is generally accepted to be the source of the turbulence needed for material to spiral inward and accrete onto the central object (Balbus & Hawley 1991). Because of the crucial role that it plays in astrophysics, there is considerable interest in trying to study the MRI in the laboratory (Rosner et al. 2004). One recent suggestion (Hollerbach & Rüdiger 2005; Rüdiger et al. 2005) involves externally imposing combined axial and azimuthal magnetic fields, which yields a new type of traveling-wave MRI. In this Letter we present experimental evidence of these traveling waves, in accordance with the theory.

The MRI is a mechanism whereby a differential rotation flow that satisfies the Rayleigh criterion, and is therefore hydrodynamically stable, may nevertheless be magnetohydrodynamically unstable. The addition of a magnetic field allows angular momentum to be transferred outward by the magnetic tension in the field lines, thereby bypassing the Rayleigh criterion, which relies on individual fluid parcels conserving their angular momentum. The MRI is particularly relevant to Keplerian flows such as those found in accretion disks, where $\Omega \sim r^{-3/2}$, which would indeed be stable according to the Rayleigh criterion.

The simplest design for attempting to reproduce the MRI in the lab is based on the familiar Taylor-Couette problem, consisting of the flow between differentially rotating cylinders. While one cannot achieve precisely a Keplerian flow profile in this problem, by appropriately choosing the rotation rates of the inner and outer cylinders one can easily achieve a Rayleigh-stable profile, which is all that is really required. By suitably adjusting the strength of an externally imposed magnetic field one should then be able to destabilize the flow again, via the MRI.

Unfortunately, the situation is not quite so simple after all. If the imposed field is purely axial (Rüdiger & Zhang 2001; Ji et al. 2001), the relevant parameter for the onset of the MRI turns out to be the magnetic Reynolds number $\mathrm{Rm} = \Omega_i r_i^2/\eta$, which must exceed $O(10)$. The hydrodynamic Reynolds number $\mathrm{Re} = \Omega_i r_i^2/\nu$ then exceeds $O(10^6)$, due to the extremely small magnetic Prandtl numbers $\mathrm{Pm} = \nu/\eta$ of liquid metals (ν is the viscosity, η the magnetic diffusivity). Such large rotation rates can be achieved, but for increasingly large Reynolds numbers end effects become increasingly important, and at $\mathrm{Re} \gtrsim O(10^6)$ may well disrupt the experiment (Hollerbach & Fournier 2004).

In contrast, if a combined axial and azimuthal field is imposed (Hollerbach & Rüdiger 2005; Rüdiger et al. 2005), the relevant parameter turns out to be Re, which must only be as large as $O(10^3)$ to obtain the MRI. These end effects are therefore less severe. The solutions in this case are also somewhat different from those for purely axial imposed fields; one obtains much the same Taylor vortices as before, but the whole pattern now drifts along the length of the cylinders (see also Knobloch 1996). This unfortunately introduces significant end effects of its own, familiar in other contexts, such as drifting dynamo waves (Tobias et al. 1998). Nevertheless, we will see that the experimental results in a bounded cylinder agree reasonably well with the theoretical results in an unbounded cylinder.

2. EXPERIMENTAL RESULTS

The experimental apparatus consists of a cylindrical annulus made of copper, with $r_i = 4$ cm, $r_o = 8$ cm, and height 40 cm. The top endplate is made of plexiglass and is stationary; the bottom endplate is made of copper and rotates with the outer cylinder. An axial magnetic field is imposed by running a current, up to 200 A, through a series of coils surrounding the entire apparatus; an azimuthal magnetic field is imposed by running a current, up to 8000 A, through a rod along the central axis. Field strengths of several hundred gauss can then be achieved, for both B_z and B_ϕ. The fluid contained within the vessel is a GaInSn alloy, having density $\rho = 6.4$ g cm^{-3}, viscosity $\nu = 3.4 \times 10^{-3}$ cm^2 s^{-1}, and magnetic diffusivity

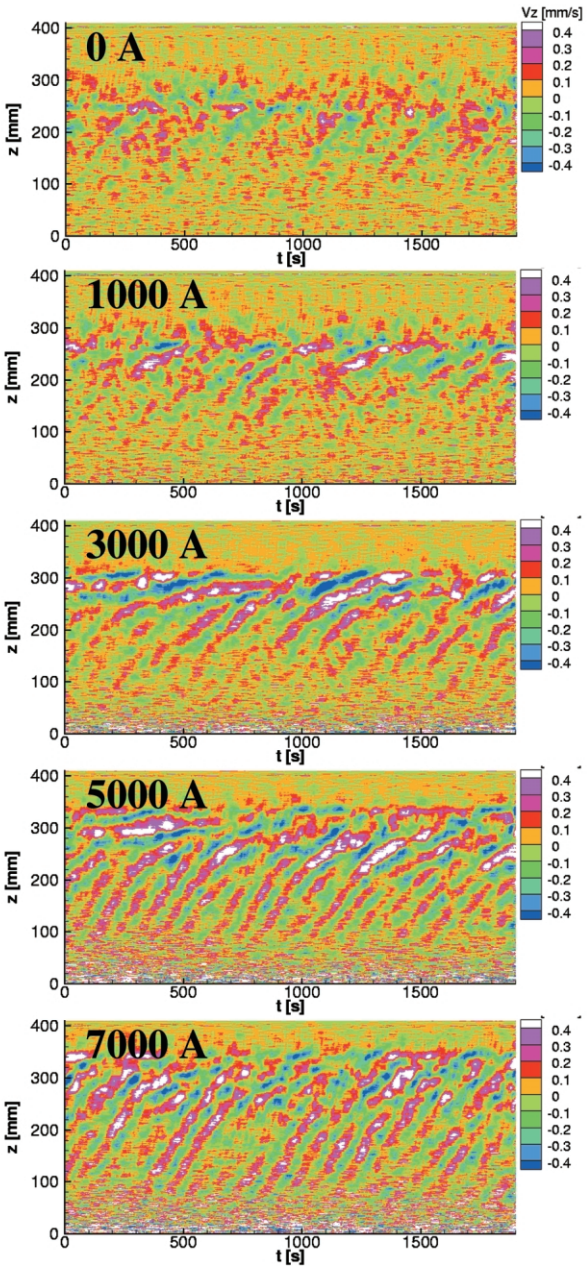

FIG. 1.—Ultrasound measurements of the axial velocity v_z, with the time average removed. Time is plotted on the horizontal axis; height along the cylinder on the vertical axis. The current along the central rod varies from 0 to 7 kA as indicated, corresponding to $B_\phi(r_i)$ up to 350 G.

$\eta = 2.4 \times 10^3$ cm^2 s^{-1}, so Pm $= 1.4 \times 10^{-6}$. Measurements were made by two ultrasonic transducers mounted on opposite sides of the top endplate, 1.5 cm from the outer wall. These provided measurements of v_z at these particular locations, along the entire 40 cm depth of the container. See also Stefani et al. (2006) for further details of the experimental setup.

For the results presented here, the rotation rates of the inner and outer cylinders were fixed at $\Omega_i = 0.377$ s^{-1} and $\Omega_o = 0.102$ s^{-1}, so $\Omega_o/\Omega_i = 0.27$, which is within the Rayleigh-stable regime $\Omega_o/\Omega_i > (r_i/r_o)^2 = 0.25$. The Reynolds number Re $= \Omega_i r_i^2/\nu = 1775$. The axial field B_z was also fixed, at 77.2 G, corresponding to a Hartmann number Ha $= B_z r_i/(\rho\mu\eta\nu)^{1/2} = 12$. The azimuthal field B_ϕ was then varied, between 0 and 350 G

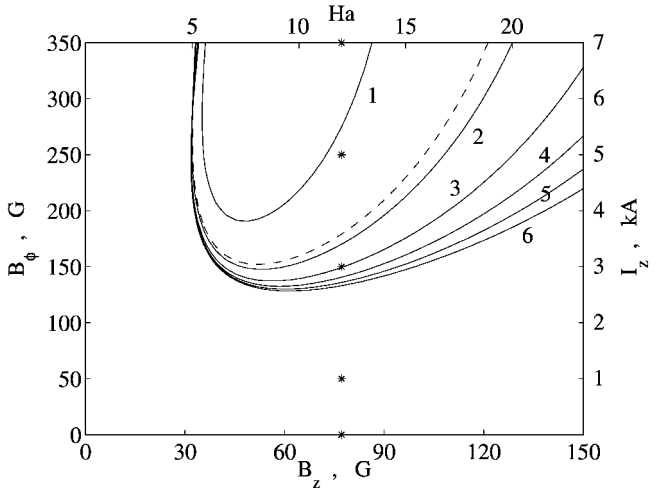

FIG. 2.—Contour plot of Re$_c$ as a function of B_z and B_ϕ. On the horizontal axes B_z is given both in gauss and in nondimensional form as Ha $= 0.1555 \times B_z$/G. On the vertical axes $B_\phi(r_i)$ is given both in gauss and in terms of the required axial current I_z. The numbers beside individual contour lines denote values from 1000 to 6000; the dashed contour line is 1775, the value used in the experiment. The five asterisks correspond to the five experimental runs in Fig. 1.

(at r_i), corresponding to electric currents up to 7000 A along the central rod.

Figure 1 shows the temporal variation of the axial velocity v_z, as a function of z along the container. The (depth-dependent) time-average has been subtracted, to remove the two Ekman vortices induced by the endplates (Kageyama et al. 2004; Hollerbach & Fournier 2004). As B_ϕ is increased, we see the gradual emergence of ever more coherent structures, drifting at speeds of 0.5–1 mm s^{-1}. Focusing attention on z between 10 and 20 cm, where the waves are most clearly defined, we obtain around 0.6 mm s^{-1} for 3 kA, and 0.8 mm s^{-1} for 5 and 7 kA. The corresponding wavelengths are 7–8 cm for 3 kA, and 5–6 cm for 5 and 7 kA. We claim that these structures are precisely the expected traveling-wave MRI.

Note though that end effects do indeed play an important role in Figure 1, for example at the upper boundary, where the waves die away some 5–10 cm from the end. Another indication of the importance of end effects, and in particular the asymmetry between the two ends, can be seen in the 0 A results: the asymmetry between top and bottom that is already visible

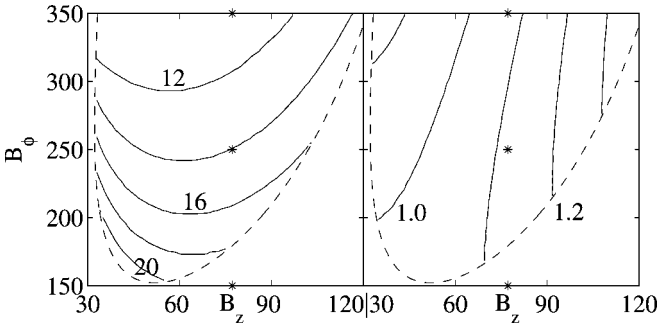

FIG. 3.—Wavelengths in centimeters (*left*) and speeds in millimeters per second (*right*) of the solutions at Re $= 1775$. As in Fig. 2, the dashed curves are the stability boundary at this particular Re. The three asterisks correspond to the three experimental runs at 3, 5, and 7 kA, where once again the wavelengths were approximately 8, 6, and 6 cm, respectively, and the speeds were 0.6, 0.8, and 0.8 mm s^{-1}.

even in this case must be caused entirely by the endplates, as a purely axial field does not distinguish between $\pm z$.

3. THEORETICAL ANALYSIS

Figure 2 shows the critical Reynolds number for the onset of this traveling-wave MRI in an unbounded cylinder, as a function of the externally imposed fields B_z and B_ϕ; these results were computed as in Hollerbach & Rüdiger (2005) or Rüdiger et al. (2005) with conducting boundary conditions. Provided $B_z > 30$ G and $B_\phi \gtrsim 150$ G, Reynolds numbers of $O(10^3)$ are already sufficient. If B_ϕ is less than 150 G, Re_c gradually rises, until for $B_\phi = 0$ we would have $\mathrm{Re}_c > O(10^6)$, the familiar result from the analysis of purely axial fields. In contrast, if B_z is less than 30 G, the instability simply ceases to exist; that is, Re_c has an essentially vertical asymptote at this boundary.

The five asterisks in Figure 2 correspond to the five plots shown in Figure 1, and the dotted contour line corresponds to the experimental value $\mathrm{Re} = 1775$. We see therefore that the experimental runs with $I_z = 0$, 1, and 3 kA should be stable, whereas the ones with 5 and 7 kA should be unstable. This is broadly in agreement with Figure 1, although there even the supposedly stable runs already show hints of traveling-wave disturbances, particularly at 3 kA. However, the waves are much more strongly developed for the 5 and 7 kA runs, as predicted by Figure 2.

Figure 3 shows the wavelengths and speeds of the unstable solutions at $\mathrm{Re} = 1775$. Wavelengths are in the range 10–20 cm, and speeds are around 1.1 mm s^{-1} (for $B_z = 77.2$ G). The speeds agree rather well with Figure 1; the experimental result that 5 and 7 kA yield virtually the same speed, 0.8 mm s^{-1}, also nicely matches the theoretical prediction that the speed should be almost independent of B_ϕ (provided B_ϕ is large enough to be in the unstable regime at all). The wavelengths do not agree quite so well; the values in Figure 1 are barely half those in Figure 3. Presumably this is again due to end effects; a 20 cm long wave certainly could not traverse a 40 cm long container without experiencing significant end effects.

4. CONCLUSION

In this Letter we have presented experimental evidence for the existence of traveling-wave disturbances in a liquid metal Taylor-Couette apparatus, and shown them to be in reasonable agreement with the theoretical predictions, particularly with regard to the wave speeds. Future experimental work will more thoroughly map out the entire B_z, B_ϕ, Ω_i, and Ω_o parameter space, as well as explore the role that different axial boundary conditions, on both the flow (Kageyama et al. 2004) and the field (Liu et al. 2006), might play. Future numerical work will similarly consider the problem in bounded cylinders, with different boundary conditions on the endplates. Only then will we fully understand what influence the endplates, and possible asymmetries between them, have on the MRI.

This work was supported by the German Leibniz Gemeinschaft, under program SAW.

REFERENCES

Balbus, S. A., & Hawley, J. F. 1991, ApJ, 376, 214
Hollerbach, R., & Fournier, A. 2004, in AIP Conf. Proc. 733, MHD Couette Flows: Experiments and Models, ed. R. Rosner, G. Rüdiger, & A. Bonanno (New York: AIP), 114
Hollerbach, R., & Rüdiger, G. 2005, Phys. Rev. Lett., 95, 124501
Ji, H. T., Goodman, J., & Kageyama, A. 2001, MNRAS, 325, L1
Kageyama, A., Ji, H. T., Goodman, J., Chen, F., & Shoshan, E. 2004, J. Phys. Soc. Japan, 73, 2424
Knobloch, E. 1996, Phys. Fluids, 8, 1446
Liu, W., Goodman, J., Herron, I., & Ji, H. T. 2006, Phys. Rev. E, submitted
Rosner, R., Rüdiger, G., & Bonanno, A., eds. 2004, AIP Conf. Proc. 733, MHD Couette Flows: Experiments and Models (New York: AIP)
Rüdiger, G., Hollerbach, R., Schultz, M., & Shalybkov, D. A. 2005, Astron. Nachr., 326, 409
Rüdiger, G., & Zhang, Y. 2001, A&A, 378, 302
Stefani, F., Gundrum, T., Gerbeth, G., Rüdiger, G., Schultz, M., Szklarski, J., & Hollerbach, R. 2006, Phys. Rev. Lett., submitted (astro-ph/0606473)
Tobias, S. M., Proctor, M. R. E., & Knobloch, E. 1998, Physica D, 113, 43